

# PROCEEDINGS OF SPIE

[SPIEDigitallibrary.org/conference-proceedings-of-spie](https://www.spiedigitallibrary.org/conference-proceedings-of-spie)

## Spectrally varying spatial frequency properties of a small pixel photon counting detector

Stefano Vespucci, Mini Das

Stefano Vespucci, Mini Das, "Spectrally varying spatial frequency properties of a small pixel photon counting detector," Proc. SPIE 10573, Medical Imaging 2018: Physics of Medical Imaging, 1057350 (9 March 2018); doi: 10.1117/12.2294975

**SPIE.**

Event: SPIE Medical Imaging, 2018, Houston, Texas, United States

# Spectrally varying spatial frequency properties of a small pixel photon counting detector

Stefano Vespucci<sup>a</sup> and Mini Das<sup>a,b</sup>

<sup>a</sup>Department of Physics

<sup>b</sup>Department of Biomedical Engineering  
University of Houston, Houston, TX 77204

## ABSTRACT

Photon counting spectral detectors (PCD) are being investigated for multiple applications such as material decomposition and X-ray phase contrast imaging. Many available detectors have fairly larger pixel sizes of about 150  $\mu\text{m}$  or larger. The imaging performance is ultimately influenced by the choice of the sensor material, pixel pitch, contact type (Ohmic or Schottkey), spectral distortions due to charge sharing and pulse pile up. Several performance aspects must be optimal including energy and spatial resolution, frequency response, temporal stability etc. to fully utilize the advantages of a PCD. For any given design, understanding the interplay of various compromising features in the detector is very important to maximize spectral capability of these detectors. In this work, we examine spatial frequency performance of a small pixel PCD such as Medipix3RX with CdTe sensors. Measurements were conducted in single pixel mode (SPM) with no charge sharing correction as well as with charge summing mode (CSM) with built in hardware based charge-sharing correction, for both fine pitch (55  $\mu\text{m}$ ) and spectroscopic (110  $\mu\text{m}$ ) modes. While most of the simulations and measurements in the past use monochromatic x-ray to investigate these spatio-energetic correlations, our work shows preliminary results on these complex correlations when a polychromatic beam is used.

**Keywords:** X-ray, Medipix, Modulation Transfer Function

## 1. INTRODUCTION

Photon counting x-ray detectors (PCDs) are being explored for an array of medical applications. These involve utilizing PCD spectral capabilities for techniques such as X-ray fluorescence (XRF), K-edge absorption, computerized tomography (CT), phase contrast and material decomposition techniques.<sup>1-8</sup> Many available detectors have fairly larger pixel sizes of about 150  $\mu\text{m}$  or larger. The imaging performance is ultimately influenced by the choice of the sensor material, pixel pitch, contact type (Ohmic or Schottkey), spectral distortions due to charge sharing and pulse pile up. Several performance aspects must be optimal including energy and spatial resolution, frequency response, temporal stability etc. to fully utilize the advantages of a PCD. Photon counting detectors (PCDs) such as Medipix3RX<sup>9,10</sup> are capable of energy discrimination and intercommunication between pixels to reduce spectral distortions. Furthermore, it allows image acquisition with zero dark noise thereby improving image quality with the potential for several low-dose medical and biological applications.

For any detector design, understanding the interplay of various compromising features in the detector is very important. In this work, we examine the spatial frequency performance of a small pixel PCD such as Medipix3RX composed of a CdTe sensors, by evaluating its response for a number of detector readout settings when using polychromatic x-ray sources.

## 2. MEDIPIX3RX DETECTOR

Medipix3RX<sup>9</sup> is a direct conversion semiconductor hybrid pixel detector developed by an international collaboration based in CERN, Geneva. The Medipix3RX structure is composed of two parts, a sensor, where the incoming photons are converted into electric signal, and the electronics, where the signal is processed for readout. The sensor usually consists of a semiconducting material such as Si, CdTe or GaAs. A grid of equally spaced metallic bump-bonds behind the sensor allows for virtual pixellation by connecting the sensor to the application specific integrated circuit (ASIC) electronics. Each bump-bond is connected to electronics allowing for independent

readout for each pixel. The Medipix3RX ASIC active area is composed of a matrix of  $256 \times 256$  pixels, each measuring  $55 \mu\text{m} \times 55 \mu\text{m}$ .

Depending on how the sensor layer is physically bond-bonded to the ASIC electronic pixels, two detector configurations are available. When each pixel of the electronics is connected to the sensor, the effective pixel size is  $55 \mu\text{m}$  and the Medipix3RX is operated in what is defined as fine pitch mode. The second configuration consists of pixels being grouped in clusters of  $2 \times 2$  pixels; here the effective pixel size is  $110 \mu\text{m}$  and each cluster becomes a single detection unit. In this configuration only one pixel per cluster is physically connected to the ASIC electronic chip. In this case Medipix3RX is operated in what is defined as spectroscopic mode. For both fine pitch and spectroscopic modes, Medipix3RX can be operated in single pixel mode (SPM) or charge summing modes (CSM).

When using a combination of fine pitch and SPM mode, each pixel works independently. Instead, by using a combination of fine pitch and CSM modes, the charge cloud deposited in any  $2 \times 2$  pixels, i.e. within an area of  $110 \mu\text{m} \times 110 \mu\text{m}$ , is reconstructed and assigned to the pixel where the highest amount of energy was deposited. This inter-pixel communication allows the correction of any spectral distortion occurring due to charge sharing. This is particularly beneficial for applications where higher detector resolution is desirable.<sup>9,10</sup> By using a combination of spectroscopic and SPM modes, each cluster ( $2 \times 2$  pixels) works independently. Using spectroscopic mode in combination with CSM mode, the charge cloud deposited in any  $2 \times 2$  cluster, i.e. within an area of  $220 \mu\text{m} \times 220 \mu\text{m}$ , is reconstructed and assigned to the cluster where the highest amount of energy was deposited. In general, for a given threshold energy  $E_i$ , the detector pixels count the number of photons having an energy above the selected threshold values. In this work, all modes described above were used to investigate the detector spatial frequency response for different imaging conditions. These studies would allow optimal acquisition conditions (energies and threshold levels) for different detector readout modes.

### 3. SLATED KNIFE-EDGE METHOD

Medipix3RX spatial frequency response was evaluated through modulation transfer function (MTF) measurements. MTF was determined by using the slated knife-edge method.<sup>11,12</sup> A steel knife edge was placed in front of the sensor, approx. 1 cm away, tilted by approx.  $10^\circ$  with respect to the detector pixels of the Medipix3RX detector. After a flat field correction, 'bad pixels' were interpolated in order for the edge not to be compromised. The result of this first step is shown in Fig. 1(a). The edge tilt angle,  $\alpha$ , is determined through Hough transformation,<sup>13</sup> which requires a binary image as an input. The latter is obtained by applying a Canny filter<sup>14</sup> to the edge image, see Fig. 1(b).

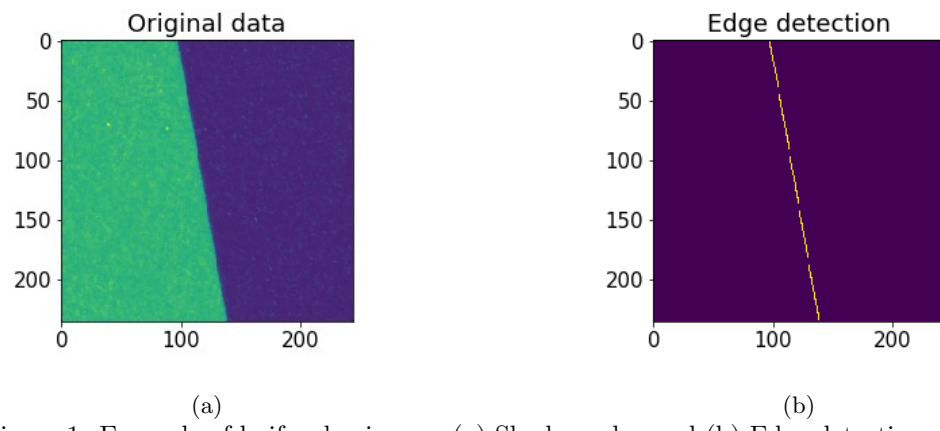


Figure 1: Example of knife-edge image. (a) Shadow edge and (b) Edge detection process.

When the edge is tilted with respect to pixels column, each pixel at the edge position is covered to a different degree by the edge itself (see points numbered from 13 to 18 in Fig.2). The line spread function obtained from an oversampled ESF was fitted with a Gaussian function before estimating the MTF for any given setting.

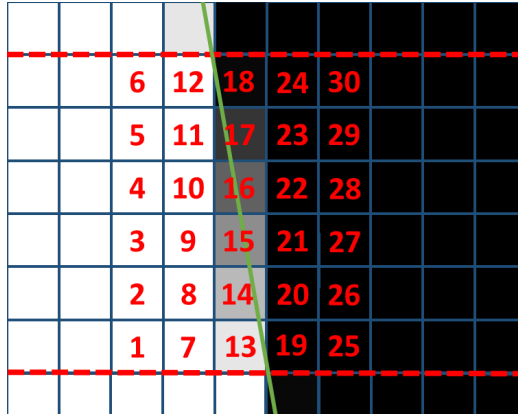


Figure 2: Illustration of the oversampling method for ESF determination.

#### 4. EXPERIMENTAL RESULTS

MTF measurements from two Medipix3RX detectors, both composed of a  $1000\text{ }\mu\text{m}$  thick CdTe sensor, operating in fine pitch ( $55\text{ }\mu\text{m}$  resolution) and spectroscopic ( $110\text{ }\mu\text{m}$  resolution) modes respectively. For all Medipix3RX modes, MTF dependence on X-ray tube energies and user specified low energy thresholds were investigated.

MTFs measured from a Medipix3RX working in a fine pitch ( $55\text{ }\mu\text{m}$ ), in both SPM and CSM modes, are shown in Fig. 3(a-b) respectively. MTF values of 10%, 30% and 70% are indicated for clarity, together with the spatial Nyquist frequency for the particular detector ( $9.1\text{ mm}^{-1}$ ). MTFs were calculated for three peak energies (40, 60 and 100 keV) at a fixed threshold level of 17 keV. Results show a general decrease in the MTF when increasing the peak photon energy. As the photon energy increases, charge sharing between pixels is larger due to bigger charge cloud produced within the sensor by photon-sensor interaction. This effectively broadens the detector LSF, with a consequent reduction in the frequency response. The effect of charge sharing is larger when using the detector in SPM, since no charge sharing correction is implemented. This is indicated by the larger variability of the MTFs over such energy range: variations in the MTFs measured in CSM are less severe. At the Nyquist frequency, decrease in the MTF,  $\Delta\text{MTF}$ , is of the order of  $\Delta\text{MTF} = 0.3$  for SPM and  $\Delta\text{MTF} = 0.12$  for CSM, when the energy is increased from 40 keV to 100 keV.

Although CSM ideally allows charge sharing effects to be corrected, it is not entirely corrected when the threshold energy is set below the x-ray fluorescence energies for Cd and Te ( $\approx 23\text{ keV}$  and  $27\text{ keV}$  respectively) from the sensor material. These photons emitted in the sensor X-ray emission lines emitted by the sensor are able, indeed, to travel distances larger than the  $55\text{ }\mu\text{m}$  (pixels pitch), reaching pixels far from the original hit, thus preventing the charge summing algorithm to correct for such energy losses.

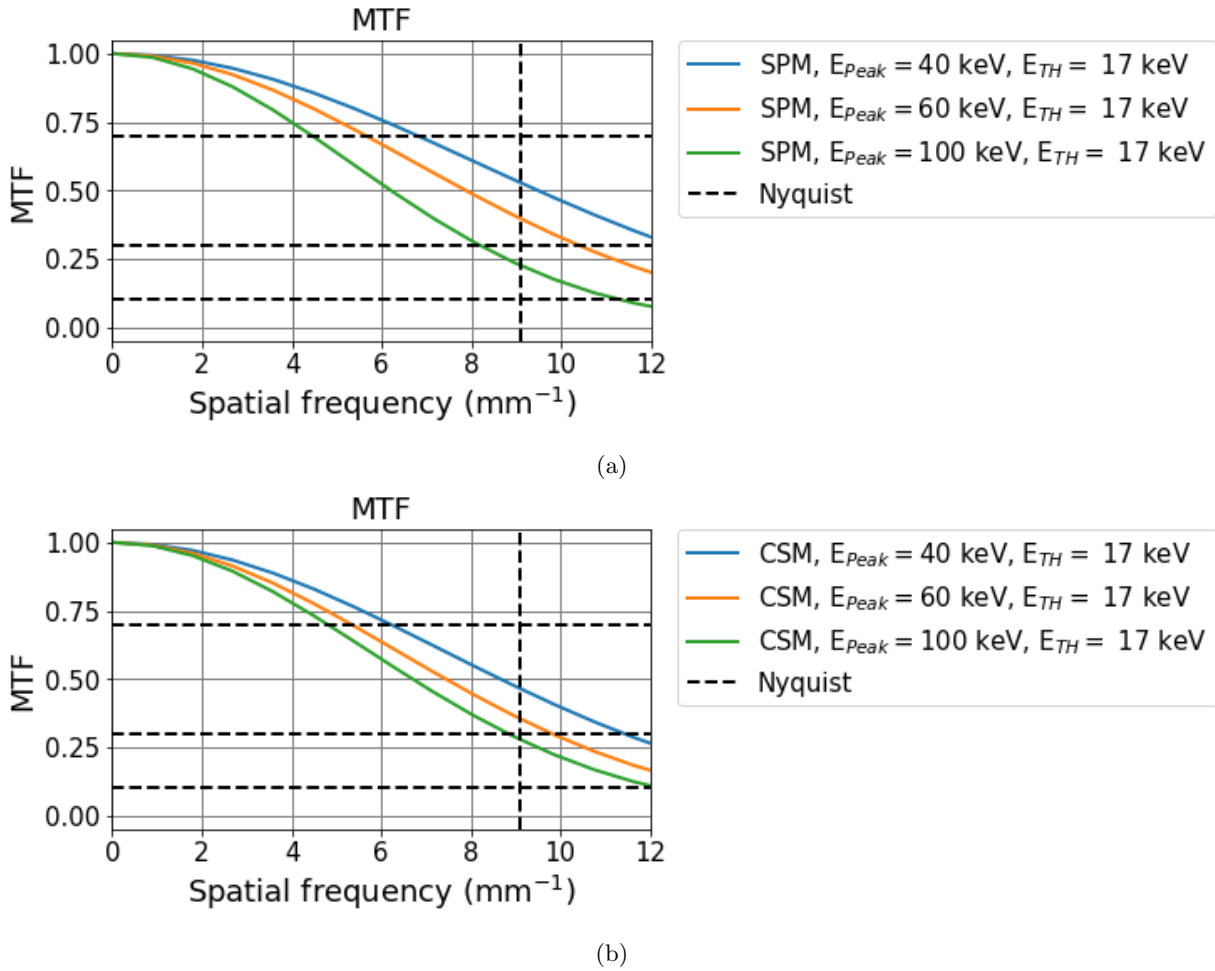


Figure 3: MTFs calculated for different peak energies at fixed threshold levels. MTFs from a 1000  $\mu\text{m}$  thick CdTe Medipix3RX, 55  $\mu\text{m}$  pitch working in (a) SPM and (b) CSM.

When using spectroscopic mode, where the pixel area is four time larger (110  $\mu\text{m} \times 110 \mu\text{m}$ ), MTF degradation due to charge sharing is thus reduced in comparison to operation in a SPM.

Figure 4 shows MTFs measured from the Medipix3RX working in spectroscopic mode, in SPM and CSM modes. The variability of the MTF between measurements at 40 keV and 100 keV are similar for SPM and CSM modes. These are of the order of  $\Delta\text{MTF} = 0.17$  and  $\Delta\text{MTF} = 0.16$  for SPM and CSM respectively.

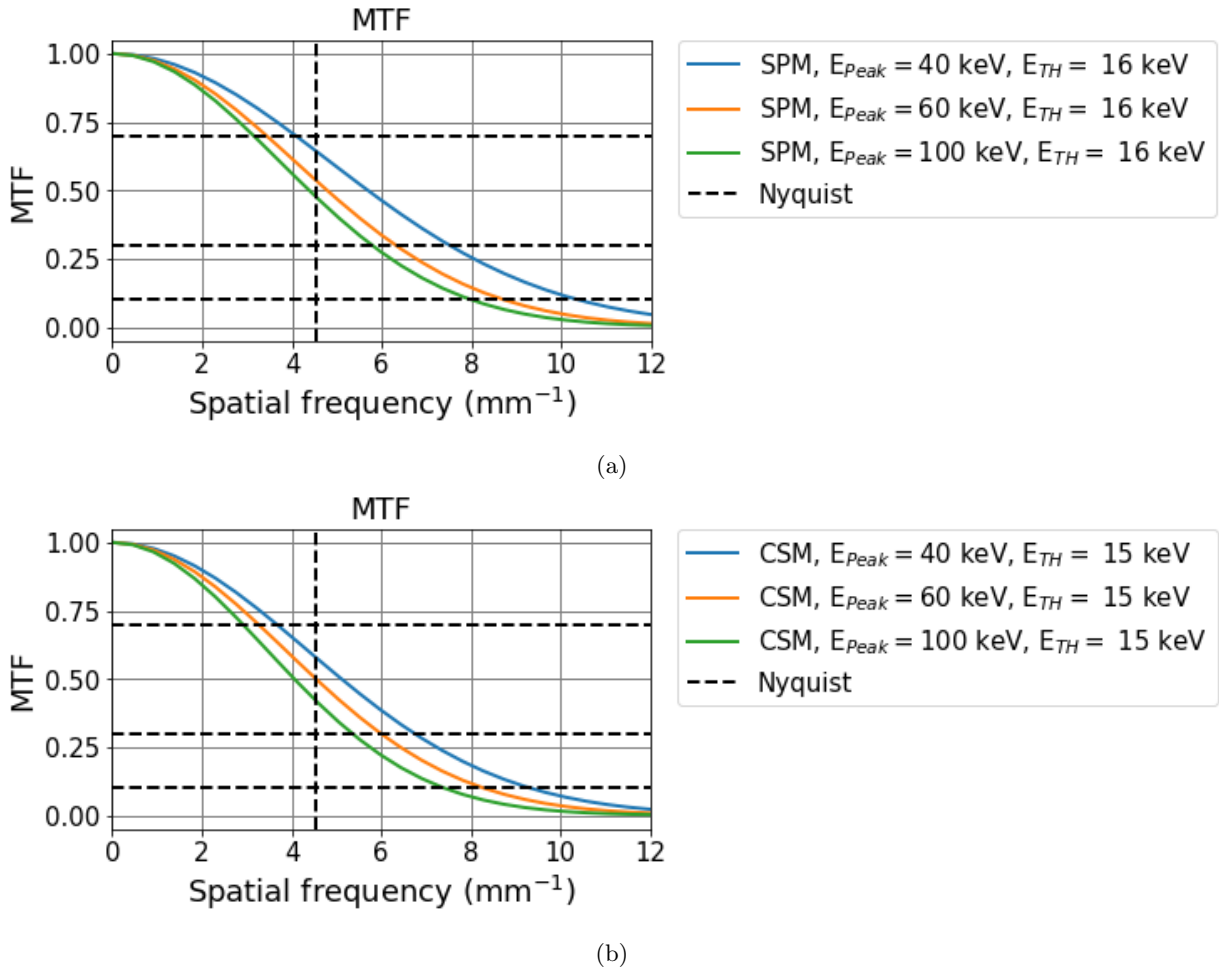


Figure 4: MTFs calculated for different peak energies at fixed threshold levels. MTFs from a  $1000 \mu\text{m}$  thick CdTe Medipix3RX,  $110 \mu\text{m}$  pitch working in (a) SPM and (b) CSM.

In general, for both fine pitch and spectroscopic modes (made exception for fine pitch SPM at 100 keV), SPM lead to an higher absolute value of the MTF at the Nyquist frequency. Difference in MTF between SPM and CSM is of the order of  $\Delta\text{MTF} = 0.06$ . This degradation might be caused by the correction scheme implemented internally by the pixels electronic within the detector.

The threshold energy dependence of MTF for a Medipix3RX working in spectroscopic mode is shown in Figure 5. An improvement in the MTF is observed when higher threshold energies are applied. In general, this trend is common for all modes of operations of Medipix3RX. In this particular case, it is possible to see how, when the threshold energy is close (26 keV) or higher (32 keV) than the energies corresponding to the x-ray fluorescence lines from the sensor material, there is a sudden increase in the absolute value of the MTFs. By doing a comparison between MTF measured at 60 keV in CSM spectroscopic mode but two different threshold energies, 15 keV (see Fig. 4(b)) and 32 keV, a  $\Delta\text{MTF} = 0.16$  is measured. To note that the improvement in the MTF is of the same order of magnitude of the one obtained when, by fixing the threshold at 16 keV, the energy is decreased from 100 keV to 40 keV, for both SPM and CSM.

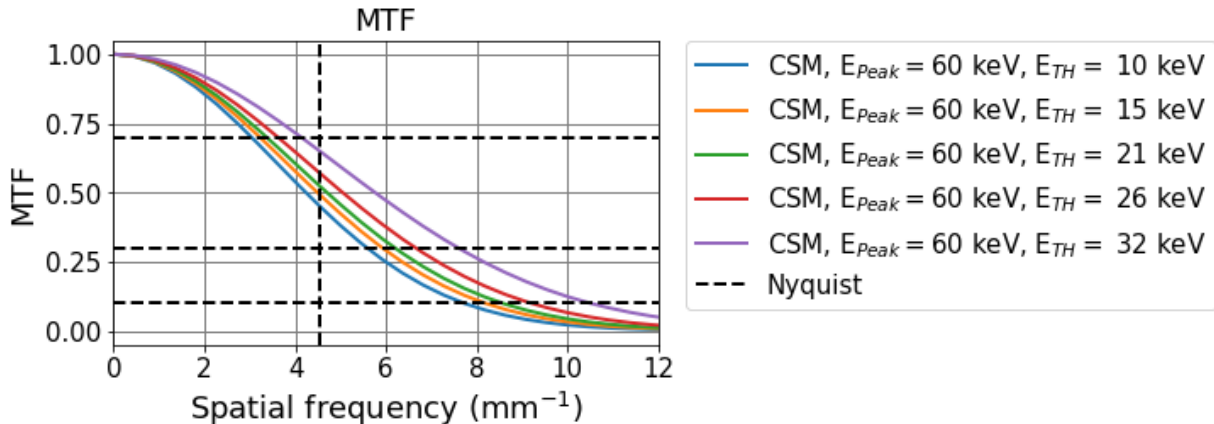


Figure 5: Calculated MTFs for a 1000  $\mu\text{m}$  thick CdTe Medipix3RX, 110  $\mu\text{m}$  pitch working in CSM. MTFs measured at 60 keV, for different threshold energies.

## 5. CONCLUSIONS

In conclusion, we performed preliminary investigations on the spatial resolution of a Medipix3RX, when using a polychromatic x-ray source. Regardless of the Medipix3RX operation mode, for a fixed threshold energy, MTF improves when lower peak x-ray energies are used. This results from the fact that lower energetic photons produce smaller charge clouds within the sensor, minimizing charge spread to neighboring pixels. When comparing fine pitch and spectroscopic modes, better spatial frequency responses for Medipix3RX are measured for fine pitch mode. However, when considering different Medipix3RX operation modes, the choice between SPM and CSM is typically not solely based on frequency response. CSM provides spectral distortion correction mechanisms which allows charge sharing to be corrected, providing better spectral responses. Aside from the spreading of primary charge cloud, X-ray fluorescence emissions within the sensor material (in our case Cd and Te) can also result in reduced MTF. These photons have a mean free path larger than our pixel pitch resulting in their energy deposited farther away from the original hit location. Since x-ray fluorescence is an isotropic process, this introduces a broadening of line spread functions, worsening the resulting MTFs. If the threshold energy is higher than the characteristic x-ray fluorescence energies from the sensor (23 keV and 27 keV for Cd and Te respectively), a sudden improvement in the MTF is visible.

Although this work provides an initial effort towards understanding the Medipix3RX spatial frequency response when a polychromatic x-ray sources is used for imaging, many aspects considering the interplay for threshold choice, sensor material, thickness, imaging energy and pitch still require further careful investigation.

## 6. ACKNOWLEDGEMENTS

We would like to thank Medipix collaboration and several members for their valuable discussions. This work was partially supported by funding from the US Department of Defense (DOD) Congressionally Directed Medical Research Program (CDMRP) Breakthrough Award BC151607 and the National Science Foundation CAREER Award 1652892.

## REFERENCES

- [1] E. Fredenberg, M. Hemmendorff, B. Cederström, M. Åslund, and M. Danielsson, “Contrast-enhanced spectral mammography with a photon-counting detector,” *Medical physics*, vol. 37, no. 5, pp. 2017–2029, 2010.
- [2] H. Ding, H.-M. Cho, W. C. Barber, J. S. Iwanczyk, and S. Molloi, “Characterization of energy response for photon-counting detectors using x-ray fluorescence,” *Medical physics*, vol. 41, no. 12, 2014.
- [3] R. E. Alvarez and A. Macovski, “Energy-selective reconstructions in x-ray computerised tomography,” *Physics in medicine and biology*, vol. 21, no. 5, p. 733, 1976.

- [4] J. P. Ronaldson, R. Zainon, N. J. A. Scott, S. P. Gieseg, A. P. Butler, P. H. Butler, and N. G. Anderson, "Toward quantifying the composition of soft tissues by spectral CT with Medipix3," *Medical physics*, vol. 39, no. 11, pp. 6847–6857, 2012.
- [5] D. Gürsoy and M. Das, "Single-step absorption and phase retrieval with polychromatic x rays using a spectral detector," *Optics letters*, vol. 38, no. 9, pp. 1461–1463, 2013.
- [6] M. Das and Z. Liang, "Spectral x-ray phase contrast imaging for single-shot retrieval of absorption, phase, and differential-phase imagery," *Optics letters*, vol. 39, no. 21, pp. 6343–6346, 2014.
- [7] K. Taguchi and J. S. Iwanczyk, "Vision 20/20: Single photon counting x-ray detectors in medical imaging," *Medical physics*, vol. 40, no. 10, 2013.
- [8] T. G. Schmidt and F. Pektas, "Region-of-interest material decomposition from truncated energy-resolved CT," *Medical physics*, vol. 38, no. 10, pp. 5657–5666, 2011.
- [9] R. Ballabriga, J. Alozy, G. Blaj, M. Campbell, M. Fiederle, E. Frojdh, E. Heijne, X. Llopert, M. Pichotka, S. Procz, *et al.*, "The Medipix3RX: a high resolution, zero dead-time pixel detector readout chip allowing spectroscopic imaging," *Journal of Instrumentation*, vol. 8, no. 02, p. C02016, 2013.
- [10] R. Ballabriga, J. Alozy, M. Campbell, E. Frojdh, E. Heijne, T. Koenig, X. Llopert, J. Marchal, D. Pennicard, T. Poikela, *et al.*, "Review of hybrid pixel detector readout ASICs for spectroscopic X-ray imaging," *Journal of Instrumentation*, vol. 11, no. 01, p. P01007, 2016.
- [11] Samei, E., Flynn, M. J., and Reimann, D. A., "A method for measuring the presampled MTF of digital radiographic systems using an edge test device," *Medical physics* **25**(1), 102–113 (1998).
- [12] T. Koenig, M. Zuber, E. Hamann, A. Cecilia, R. Ballabriga, M. Campbell, M. Ruat, L. Tlustos, A. Fauler, M. Fiederle, *et al.*, "How spectroscopic x-ray imaging benefits from inter-pixel communication," *Physics in medicine and biology*, vol. 59, no. 20, p. 6195, 2014.
- [13] R. Duda, O. Richard and P. E. Hart, "Use of the Hough transformation to detect lines and curves in pictures," *Communications of the ACM*, vol. 15, no. 1, pp. 11–15, 1972.
- [14] J. Canny "A computational approach to edge detection," *Readings in Computer Vision*, pp. 184–203, 1987.
- [15] K. Taguchi, E. C. Frey, X. Wang, J. S. Iwanczyk, and W. C. Barber, "An analytical model of the effects of pulse pileup on the energy spectrum recorded by energy resolved photon counting x-ray detectors," *Medical physics*, vol. 37, no. 8, pp. 3957–3969, 2010.
- [16] E. Frojdh, R. Ballabriga, M. Campbell, M. Fiederle, E. Hamann, T. Koenig, X. Llopert, D. de Paiva Magalhães, and M. Zuber, "Count rate linearity and spectral response of the Medipix3RX chip coupled to a 300 $\mu$ m silicon sensor under high flux conditions," *Journal of Instrumentation*, vol. 9, no. 04, p. C04028, 2014.